

CRASH COMPATIBILITY OF AUTOMATED VEHICLES WITH PASSENGER
VEHICLES

A Thesis

by

ANIRUDDHA ZALANI

Submitted to the Graduate and Professional School of
Texas A&M University
in partial fulfillment of the requirements for the degree of

MASTER OF SCIENCE

| | |
|---------------------|-----------------------------|
| Chair of Committee, | Anastasia Hanifah Muliana |
| Committee Members, | Chiara Silvestri Dobrovolny |
| | Stefan Hurlebaus |
| | Marcia A. Cooper |
| Head of Department, | Guillermo Aguilar |

December 2021

Major Subject: Mechanical Engineering

Copyright 2021 Aniruddha Zalani

ABSTRACT

Automated Vehicles have been one of the most sought-after concepts to make transportation more effective and safer. One such class of vehicles is the no-occupant vehicles with automated driving systems (ADS), which are primarily intended for goods transportation services. This vehicle class presents a body structure different than that of a passenger vehicle. Yet, these no-occupant automated vehicles are sharing the roads and could potentially be involved in crashes with passenger vehicles. Occupant safety can be compromised if vehicles are not compatible from a crashworthiness perspective. ADSs vehicles should consider appropriate vehicle crashworthiness compatibility given the potential for interactions with vulnerable road users and other vehicle types.

Investigation of the level of automated vehicle crashworthiness compatibility with human-driven vehicles can lead to more appropriate vehicle designs, as well as more suitable and better passive protection systems for occupants in such crash scenarios. This research project considers finite element crash computer simulation investigation between ADS and passenger vehicles with the intent to provide a better understanding of the differences in crashworthy behavior of ADS vehicles.

ACKNOWLEDGEMENTS

I would like to thank my committee chair, Dr. Muliana, and my committee members, Dr. Chiara, Dr. Hurlebaus and Dr. Cooper, for their guidance and support throughout the course of this research.

Texas A&M university High Performance Research Computer super computers were used to carry out Finite element simulations. The FEM vehicle models were utilized from the George Mason University's Center for Collision Safety (CCSA).

This project was funded by the Safety through Disruption (Safe-D) National University Transportation Center, a grant from the U.S. Department of Transportation – Office of the Assistant Secretary for Research and Technology, University Transportation Centers Program.

CONTRIBUTORS AND FUNDING SOURCES

Contributors

This work was supervised by a thesis committee consisting of Professor Muliana and Chiara Silvestri Dobrovolny of the Department of CVEN.

All other work conducted for the thesis was completed by the student independently.

Funding Sources

Graduate study was supported by a fellowship from Safety through Disruption (SAFE-D) National University Transportation Center.

NOMENCLATURE

| | |
|---------|--|
| IIHS | Insurance Institute for Highway Safety |
| FMVSS | Federal Motor Vehicle Safety Standards |
| NHTSA | National Highway Traffic Safety Administration |
| CCSA | Center for Collision Safety Analysis |
| CG | Center of Gravity |
| FEA | Finite Element Analysis |
| FSM | flail space model |
| LS-DYNA | An advanced general-purpose multiphysics simulation software |
| MASH | Manual for Assessing Safety Hardware |
| NCAC | National Crash Analysis Center |
| OIV | Occupant Impact Velocity |
| ORA | Occupant Ridedown Acceleration |
| TRAP | Test Risk Assessment Program |
| TTI | Texas A&M Transportation Institute |
| g | gravity |

TABLE OF CONTENTS

| | Page |
|--|------|
| ABSTRACT | ii |
| ACKNOWLEDGEMENTS | iii |
| CONTRIBUTORS AND FUNDING SOURCES..... | iv |
| NOMENCLATURE..... | v |
| TABLE OF CONTENTS | vi |
| LIST OF FIGURES..... | viii |
| LIST OF TABLES | ix |
| CHAPTER I INTRODUCTION | 1 |
| CHAPTER II BACKGROUND..... | 3 |
| Frontal Impact Between Two Passenger Vehicles..... | 3 |
| What is a crumple zone? | 3 |
| What does NHTSA suggest?..... | 5 |
| Insurance Institute for Highway Safety (IIHS) Crash Testing Procedures | 5 |
| Side Impact Crashworthiness Evaluation (SICE) | 6 |
| Frontal Overlap Testing Criteria | 8 |
| Roadside Safety Features Crash Testing Guidelines..... | 12 |
| MASH Flail-Space Model..... | 12 |
| Non-Occupant Automated Vehicle Descriptions | 14 |
| CHAPTER III METHOD..... | 17 |
| Identified Critical Crash Scenarios | 17 |
| Finite Element Vehicle Models..... | 20 |
| CHAPTER IV RESULTS | 24 |
| Side Impact Simulation..... | 24 |
| Deformations of B-Pillar and Mid-AB Pillar | 24 |
| Frontal Impact Simulations | 32 |
| Moderate and Small Overlap Impact Simulations | 32 |

| | |
|-----------------------------|----|
| CHAPTER V CONCLUSIONS | 37 |
| Discussion | 37 |
| Recommendations | 39 |
| REFERENCES | 41 |

LIST OF FIGURES

| | Page |
|---|------|
| Figure 1. Rendering of Automated Vehicle on the Streets..... | 2 |
| Figure 2. Frontal Passenger Impact..... | 3 |
| Figure 3. Crumple Zone | 4 |
| Figure 4. Side Impact Configuration (Reprinted from [iihs.org] [8]) | 7 |
| Figure 5. Intrusion Criteria (Reprinted from [iihs.org] [9][10])..... | 8 |
| Figure 6. Front Impact Configurations (Reprinted from [9][10]) | 9 |
| Figure 7. Corresponding Measuring Locations (Reprinted from [iihs.org] [9]) | 11 |
| Figure 8. Front Intrusion Criteria (adapted from [iihs.org] [9][10]) | 12 |
| Figure 9. Overall Research Methodology | 17 |
| Figure 10. Impacting Locations | 18 |
| Figure 11. Case 1. Moderate Overlap Arrangement | 19 |
| Figure 12. Case 2. Small Overlap Arrangement | 20 |
| Figure 13. General development of no-occupant ADS vehicle [Reprinted from [18]].... | 21 |
| Figure 14. Energy Curve | 22 |
| Figure 15. Measurement Locations For B-Pillar and AB Pillar..... | 24 |
| Figure 16. Pre-Impact Vehicle Image | 25 |
| Figure 17. Pre-Impact Image..... | 32 |
| Figure 18. TRAP Coordinate System..... | 35 |

LIST OF TABLES

| | Page |
|--|------|
| Table 1. Current/Prototype ADS Vehicles | 15 |
| Table 2. Finite Element Vehicle Models..... | 23 |
| Table 3. Post Impact Images of B- Pillar and AB pillar | 25 |
| Table 4. B- and Mid AB-Pillar deformation values | 30 |
| Table 5. AB Pillar door intrusion area | 30 |
| Table 6. Post Impact Images of Small and Moderate Overlap..... | 33 |
| Table 7. Small Overlap OIV and Ride Down Acceleration values..... | 35 |
| Table 8. Moderate Overlap OIV and Ride Down Acceleration values..... | 35 |
| Table 9. Small Overlap Intrusion Measurements | 36 |
| Table 10. Moderate Overlap Intrusion Measurements..... | 36 |

CHAPTER I

INTRODUCTION

Automated vehicles have been one of the most sought-after advancements in the automotive field. Ever since self-driving vehicles started to appear on the roadways it has been a goal of vehicle manufacturers to have more and more automated vehicles with minimum human intervention. One such category of vehicles is the no-occupant delivery vehicles equipped with Automated Driving System (ADS). These vehicles are primarily used to transport goods ranging from delivery/pizza boxes to large blocks of wooden logs. One of the striking features for such vehicles is the absence of driver /occupants, steering wheel, and of an occupant compartment. In the United States, vehicles need to meet certain federal regulatory standards, such as those mandated by the Federal Motor Vehicle Safety Standard (FMVSS), [1]. ADS vehicles may not need to undergo such tests, since they do not have an occupant compartment. It is necessary, however, to understand the compatibility of these ADS vehicles with regular passenger vehicles in the event of an impact. This study focuses on the use of crash impact guidelines set by the Insurance Institute for Highway Safety (IIHS) to better investigate the need of evaluating the crashworthiness compatibility between such vehicle class types.



Figure 1. Rendering of Automated Vehicle on the Streets

CHAPTER II
BACKGROUND

Frontal Impact Between Two Passenger Vehicles

Since the dawn of the automobile era, vehicle collisions have been a commonly occurring phenomenon. Figure 2 illustrates a computer simulation replica of a frontal crash between two passenger vehicles of similar size and type.

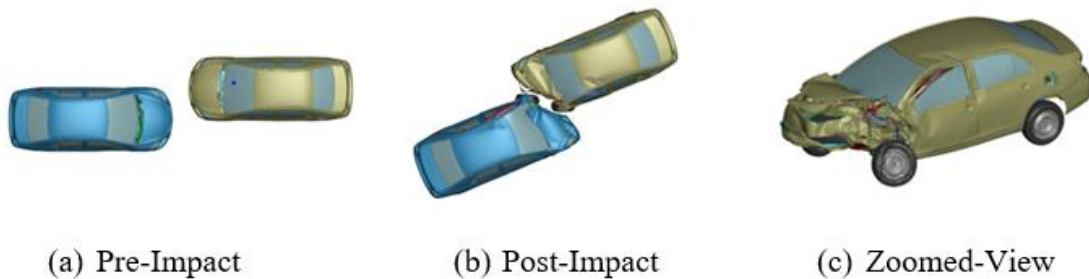


Figure 2. Frontal Passenger Impact

What is a crumple zone?

The crumple zone is the area in the front and back of a vehicle that is designed to absorb impact energy in the event of a collision, which translates to a minimization of occupant forces and potential injuries. Depending on the vehicle manufacturer a crumple zone can either be built up of frames or specialized metals which are designed to impart structural integrity and easily crush in the event of a crash.

Based on the mass, speed, and structure of the vehicle, large amount of forces are involved in a collision. This is measured in the form of deceleration of the impacting vehicle. This crumple zone distributes the amount of the deceleration on the vehicle's

body before it is transmitted to the passengers by creating a buffer zone [2]. During the impact, some parts such as engine room and the occupant compartment are stiffer and hence experience minimum deformation. Most of the impact energy is absorbed by this crumple zone. For instance, if the vehicle hits a stationary object such as light pole or a tree, this force gets transmitted to those objects. If the vehicle strikes another stationary vehicle, the crumple zone of the impacted vehicle would absorb some of the decelerating forces.

As shown in Figure 3, a typical passenger vehicle has two crumple zones - one in the front and the other in the back. The middle section is the occupant compartment. However, a small size ADS vehicle, for example, does not have a crumple zone, as it lacks a passenger compartment. Most of this type of ADS vehicle consists of cargo space with boxes, for goods delivery. Being electric in nature, these ADS vehicles do not have engine compartment, but an electric motor and a battery pack instead.



Figure 3. Crumple Zone

Automation of vehicles is one of the exciting innovations in the transportation sector. This promising sector has the potential to reduce highway fatalities and injuries as 94% of the crashes occur due to human error [3]. Although the modern automated vehicles are equipped with state-of-the-art sensors and cameras to make these vehicles

safer, a question mark remains related specifically to the safety and reliability of such level 4 /5 vehicles (those that require very little to no-human assistance). A recent study [4] conducted by the Insurance Institute for Highway Safety (IIHS) suggests automated vehicles would be able to avoid only one third of crashes caused by human error. Based on 5,000 crashes, the team assumes the crashes will be due to perception or performance errors [4]. There have been various accidents associated with automated vehicles and some even proved to be fatal.

What does NHTSA suggest?

The National Highway Traffic Safety Administration (NHTSA) believes ADS's can significantly improve the roadway safety in the United States. One of the key ADS safety elements as presented in NHTSA's *Automated Driving Systems – A Vision for Safety* is crashworthiness compatibility and occupant protection [3]. Since the ADS's will be operating among other passenger vehicles vehicle manufacturers need to consider the possibility of a crash occurrence and the safety of the passengers. As stated in [3], "Unoccupied vehicles equipped with ADSs should provide geometric and energy absorption crash compatibility with existing vehicles on the road. ADSs intended for product or service delivery, or other unoccupied use scenarios should consider appropriate vehicle crash compatibility given the potential for interactions with vulnerable road users and other vehicle types [3]".

Insurance Institute for Highway Safety (IIHS) Crash Testing Procedures

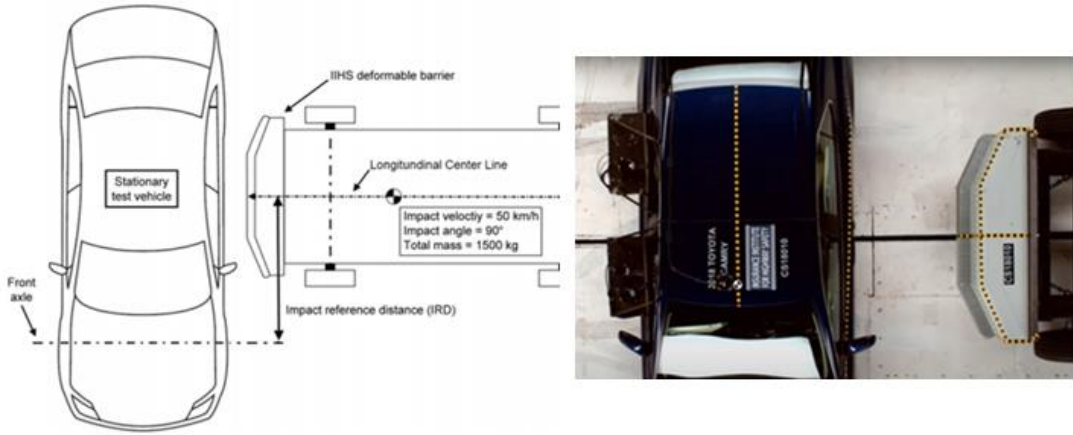
The IIHS is a nonprofit organization that focuses on highway safety. Its research focuses on reducing injuries, fatalities, and motor vehicle damages. The Vehicle Research Center (VRC) of the Institute studies vehicles crashworthiness and rates it based on the results of specific full-scale tests conducted in house [5]. The Institute has test protocols for a variety of full-scale crash testing, including:

- Moderate Frontal Overlap
- Small Frontal Overlap
- Side Impact Testing
- Rear impact and head restraint - This test is used to calculate head injuries in a rear impact. A whiplash test with a BioRID impact dummy is kept on a sled and is moved to replicate a rear-end collision. Ratings are given to the head restraint to determine the acceptable values.
- Roof strength - This test is a measure of how strong the roof of a vehicle is in case a rollover occurs. Although passive restraint systems such as side airbags and seat belt help protect the occupants still can incur an injury. In this test a metal plate is made to push inside the roof to measure the amount of force needed to crush the roof. This force is divided by the vehicle's weight to calculate strength to weight ratio. Based on the number the vehicle is given a rating of either good, acceptable, marginal or poor.

Considering the resources available to this project, only frontal and side impact tests were considered.

Side Impact Crashworthiness Evaluation (SICE)

The IIHS side impact tests were developed in 2003 using a Movable Deformable Barrier (MDB) impacting a stationary passenger vehicle. The impacting MDB barrier has a mass of 1,500 kg (3300 lbs), and a nominal speed and angle of 50 km/h (31 mph) and 90 degrees, respectively. The test vehicle and its properties represent those of a mid-size Sports Utility Vehicle (SUV) [6]. In October 2020, the organization developed a new barrier with a slight heavier mass and high-speed velocity [7]. The impact location remains the same. The Impact Reference Distance (IRD) is defined based on the test vehicle as (also shown



[Reprinted from [iihs.org]]:

$$IRD = \begin{cases} 144.8 \text{ cm} & \text{wheelbase} < 250 \text{ cm} \\ (wheelbase \div 2) + 19.8 \text{ cm} & 250 \text{ cm} \leq wheelbase \leq 290 \text{ cm} \\ 164.8 \text{ cm} & wheelbase > 290 \text{ cm} \end{cases} \quad [8]$$

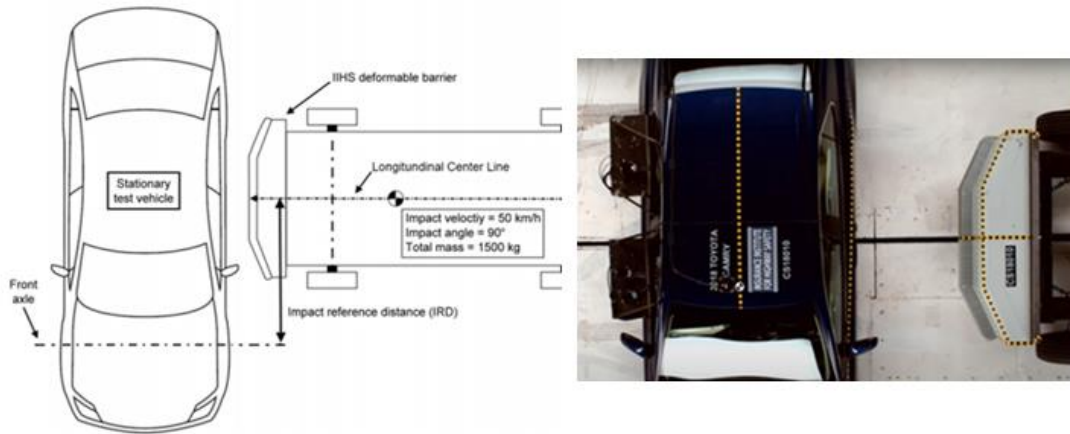


Figure 4. Side Impact Configuration (Reprinted from [iihs.org] [8])

It is important to note here that the impact location for the impacting vehicle is the B-pillar of the impacted vehicle. The MDB barrier strikes the vehicle to maximize loading to the occupant compartment. However, the IIHS [8] reports that “Currently, there is no set alignment rule for vehicles that fall into this category, therefore impact alignment is determined on a case-by-case basis.”

Figure 5 [Reprinted from [iihs.org]] illustrates the intrusion criteria developed by the IIHS as part of the evaluation process for these full-scale crash tests. The differences between pre- and post-deformation from the location of the seat centerline to that of the B-Pillar is evaluated to determine the structural rating associated with the performance of the vehicle.

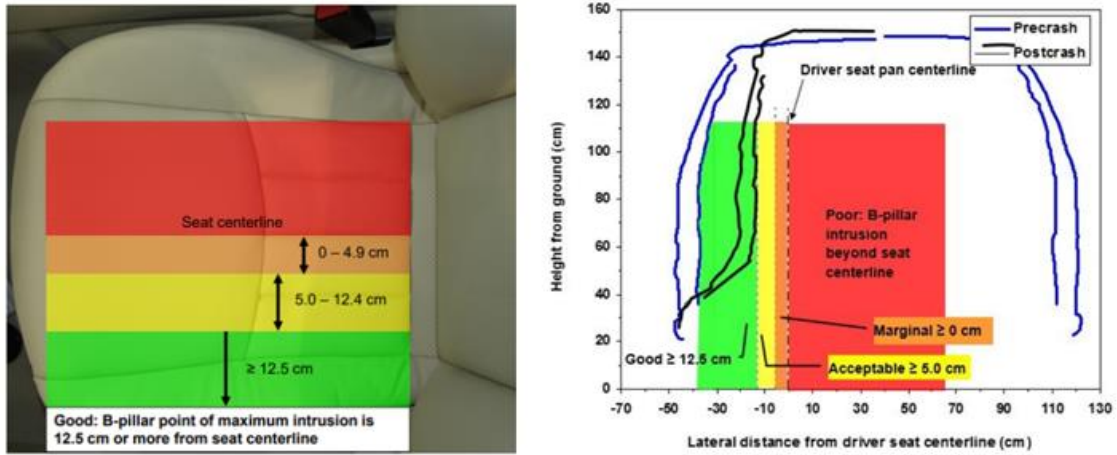


Figure 5. Intrusion Criteria (Reprinted from [iihs.org] [9][10])

Frontal Overlap Testing Criteria

The IIHS has two modes for frontal impact tests: moderate overlap and small overlap.

Moderate Overlap tests help determine how restraint systems (seatbelts and airbags) perform during a crash. The testing procedure involves a vehicle striking a stationary 2-foot-tall aluminum honeycomb deformable barrier. A Hybrid III 50th percentile male dummy is positioned on the driver seat of the vehicle. The vehicle strikes the deformable barrier at a location corresponding to the 10% of the test vehicle width, as represented in Figure 6a [Reprinted from [iihs.org]]. The forces experienced during this test are representative of two similar mass vehicles travelling towards each other, just undergoing 65 km/hr (40 mph) each [5].

Small Overlap tests determine the structural integrity of the vehicle cage and the energy absorbed by the vehicle crush zones. The testing procedure involves the vehicle impacting a 5-foot-tall rigid barrier at a location corresponding to the 25% of the test

vehicle width, as represented in Figure 6b [Reprinted from [iihs.org]]. A 50th percentile Hybrid III male dummy is placed on the driver seat of the vehicle. This crash represents the case of a vehicle striking a pole or a tree [5].

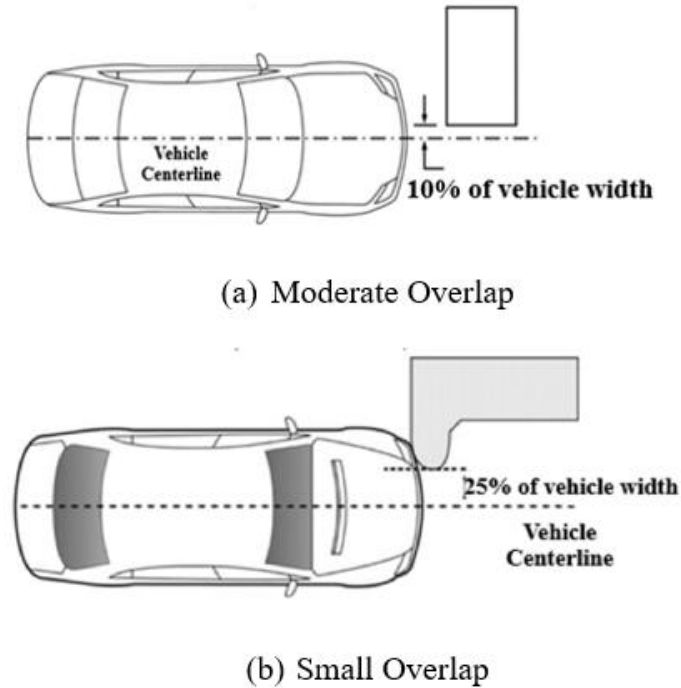


Figure 6. Front Impact Configurations (Reprinted from [9][10])

Measurement Locations

One of the frontal measurement criteria is based on the calculation of the deformation of interior components, just in front of the anthropomorphic device. Based on the type of frontal crash test considered, the difference between pre and post impact distance is measured to see what ratings the vehicle falls into, for such test [9][10].

Figure 7 [Reprinted from [iihs.org]] shows the comparison of the measurement locations inside of the actual vehicle with the FEM model used in this study for determining the

intrusion locations. The images on the right are zoomed in view of the locations for a clear understanding.

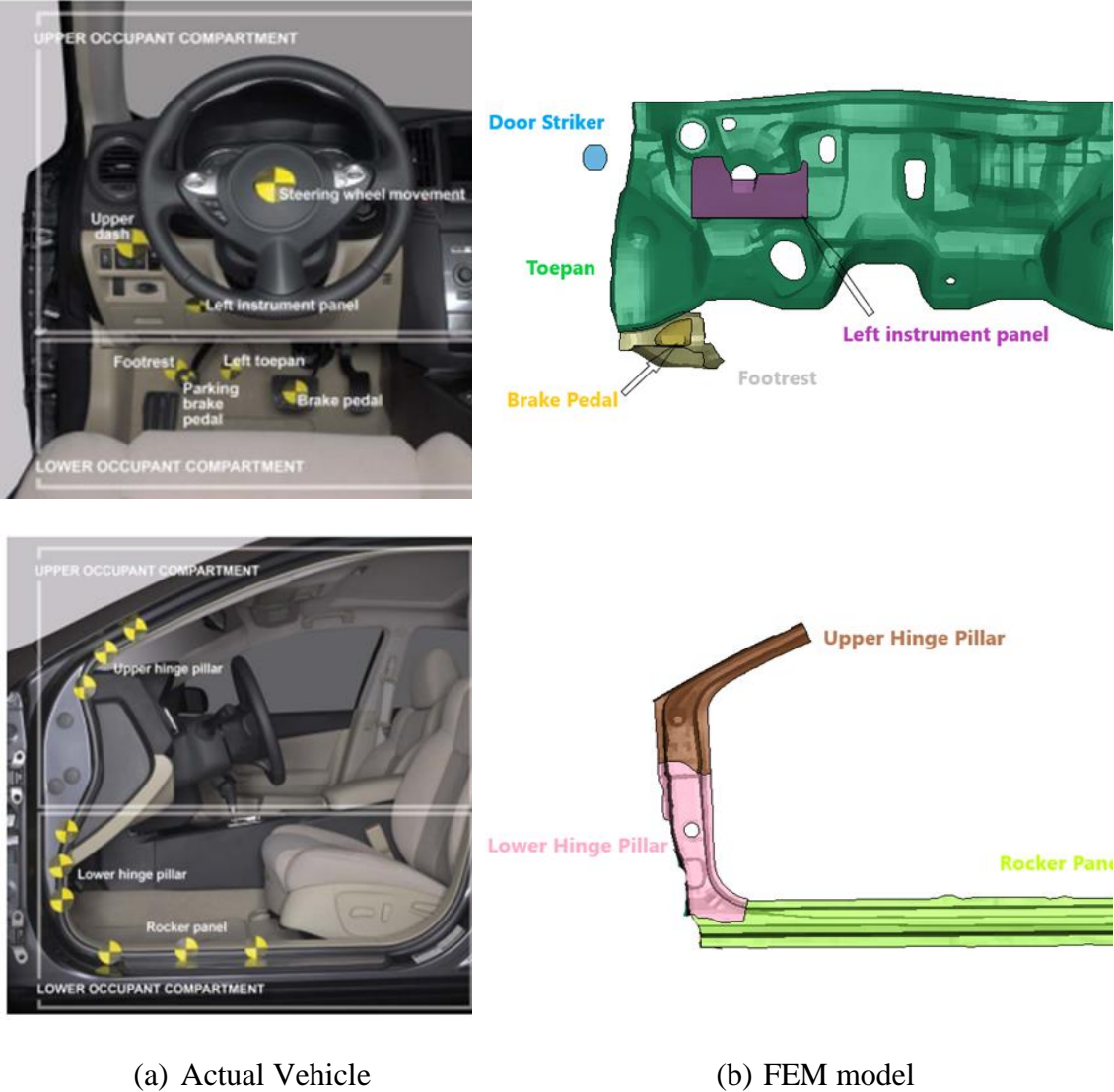
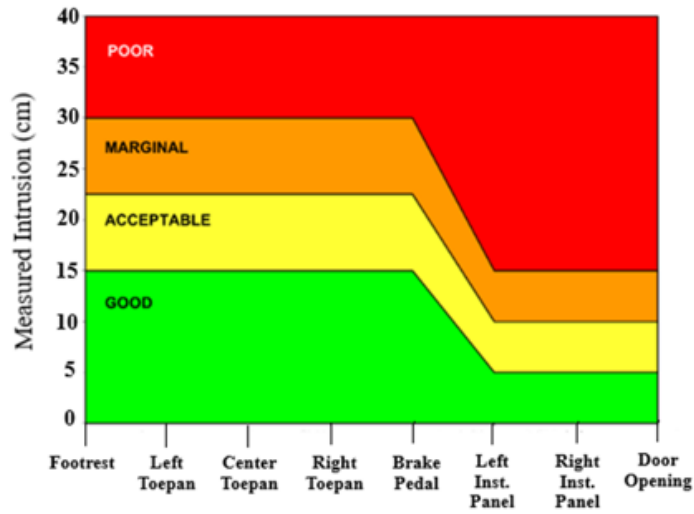
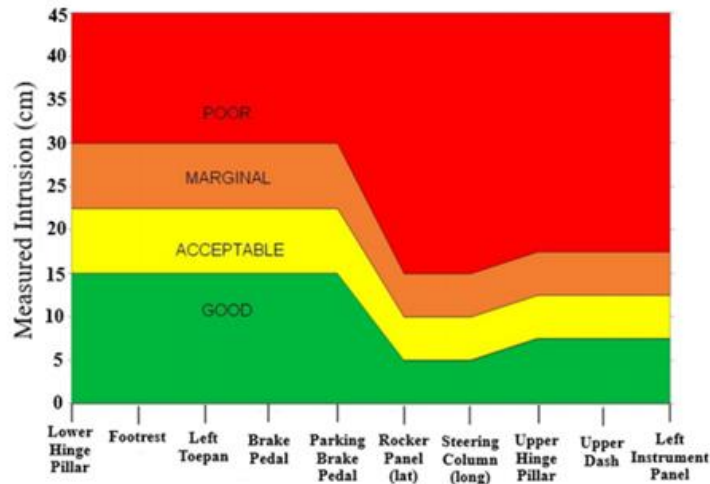


Figure 7. Corresponding Measuring Locations (Reprinted from [ihs.org] [9])

Figure 8 [adapted from [ihs.org] [9][10] represents the intrusion measurement criteria for the small and moderate overlap tests. These distances are measured from the driver door striker to the concerned locations.



(a) Moderate Overlap



(b) Small Overlap

Figure 8. Front Intrusion Criteria (adapted from [ihs.org] [9][10])

Roadside Safety Features Crash Testing Guidelines

Full-scale crash testing is used to assess vehicle crashworthiness. The Manual for Assessing Safety Hardware (MASH) guidelines includes two main evaluation criteria are used within MASH to evaluate the results of a roadside safety crash testing: structural adequacy and occupant injury risk. The risk of occupant injury also depends on the crashworthiness of the impacting vehicle, which relates to the design of the occupant compartment, structural integrity, padding, restraint conditions, etc. Occupant injury risk is evaluated in MASH using vehicle dynamics and accelerations during and after impact, through the adoption of the Flail-Space Model (FSM) [11].

MASH Flail-Space Model

The FSM [11] estimates the average deceleration that an unrestrained occupant would experience when contacting the vehicle interior during an impact event for evaluation of occupant impact velocity (OIV) and occupant ridedown acceleration (RDA), which are used for assessing the injury criteria of an occupant.

To simplify the application of FSM to a full-scale crash testing, the occupant is modeled as an unrestrained point mass that can move as a free missile [11]. The OIV with the vehicle interior at the point when the free body traverses 0.6 m longitudinally, and 0.3 m laterally is used to assess the injury criteria of the occupant. The FSM does not consider vertical accelerations of the vehicle and the occupant is assumed to be a 50th percentile male.

These assumptions provide some limitations in the use of FSM and may cause the results to be overly- conservative. OIV and RDA are calculated based on the injury scale

set by the American Association for Automotive Medicine (AAAM) which classifies an individual injury according to its relative severity on a 6-point scale. The upper limit for occupant protection falls under the code 3 and 4 per the Federal Motor Vehicle Safety Standards (FMVSS) No. 208, which means the injury can be serious but not life threatening. The threshold limit for OIV was set at 12 m/s based on the head impact of the occupant with the windshield that ranges from 13–16 m/s and head injury criteria (HIC) of 1000 per FMVSS No. 208. Further occupant injury depends on the magnitude of this acceleration. A threshold RDA value of 20.49 g is applicable in both longitudinal and lateral directions [13].

These criteria mentioned in the sections above are applicable to crashes involving passenger vehicles. However, the question arises whether these criteria are still applicable for crashes involving no-occupant automated vehicles impacting passenger vehicles, considering:

- a. ADS vehicles have no crumple zone - all the impacting energy during a crash transfer to the passenger vehicle.
- b. The differences in geometry and dimensions between the no-occupant automated vehicle and the passenger vehicle.
- c. ADS vehicles are full electric. The presence of a battery /motor increases the vehicle mass compared to that of a combustion engine vehicle.

With these considerations, there are two main objectives of this research

- (a) To investigate whether these criteria are still applicable for no-occupant automated vehicles.

(b) If yes, is there other potential impacting location that can be considered critical.

Non-Occupant Automated Vehicle Descriptions

The Covid-19 pandemic has made the need for automated delivery vehicles equipped with ADS technology even more in demand and convenient. Transportation of goods and other services were greatly disrupted due to the non-availability of human drivers. A no-occupant automated vehicle can be used for delivery and therefore can help in reducing the spread of the virus and make delivery more accessible to consumers.

These no-occupant automated vehicles are designed to operate with zero human assistance and are currently being used for both human transport and goods delivery. Although there are various organizations that are actively working on the concept of fully automated electric vehicles, Nuro is one such company that has been in operation and has been approved for deployment in States such as California and Texas. In 2018, NHTSA approved a temporary exemption from certain FMVSS rules such as rearview mirrors and windshields for Nuro vehicles, for the first 5000 vehicles and for a two-year testing period [14]. These vehicles have been employed for grocery deliveries in Texas and California. Companies such as Dominos and Walmart have also began using this service for their delivery operation. General Motors is also launching Chevrolet Bolt for similar operation and has requested 16 FMVSS exemptions from NHTSA, including exemptions from side impact protection testing.

Table 1. Current/Prototype ADS Vehicles

| Vehicle Name | Vehicle Description | Vehicle Image |
|------------------|---|---|
| Nuro R2 [15] | <ul style="list-style-type: none"> • Driverless electric ADS vehicle for goods delivery with NHTSA exemption. • Currently in operation in Houston and California • Use: grocery delivery and domino’s pizza. • No occupant compartment. • Dimensions - 2.74*1.1*1.86 (m)[L*B*W] • Max Speed – 40 km/hr. (25 mph) • Total Vehicle Weight – 1,340 kg (2900 lb.) |  <p data-bbox="1089 569 1414 596">NURO R2[Reprinted from [15]</p> |
| Einride Pods[16] | <ul style="list-style-type: none"> • Originally known as T-pods these level 4 electric automated trucks are made by Einride AB. • No occupant compartment. • Started delivering goods in middle of 2019 with a max allowable speed of 3 mph and can reach up to 19 mph [16]. • Payload capacity – 16 tons • Total mass - 52 tons • Newer Automated Electric Transport (AET) - AET 3 and AET 4 with same capacity can reach up to 45 km/hr. (28 mph) and 85 km/hr.(53mph), respectively. |  <p data-bbox="1073 911 1430 938">Einride Pod [Reprinted from [16]</p> |
| Zoox [17] | <ul style="list-style-type: none"> • No driver compartment. • Intended to be used for both passengers and goods. • Dimensions – 3.63 * 1.72 * 1.94 m [L*B*W] • Max Speed – 120 km/hr. (75 mph) • Weight – 2500 kg (5,400 pounds) |  <p data-bbox="1105 1226 1398 1253">ZOOX [Reprinted from [17]</p> |

CHAPTER III

METHOD

Figure 9 highlights a flowchart for the overall methodology followed in the project.

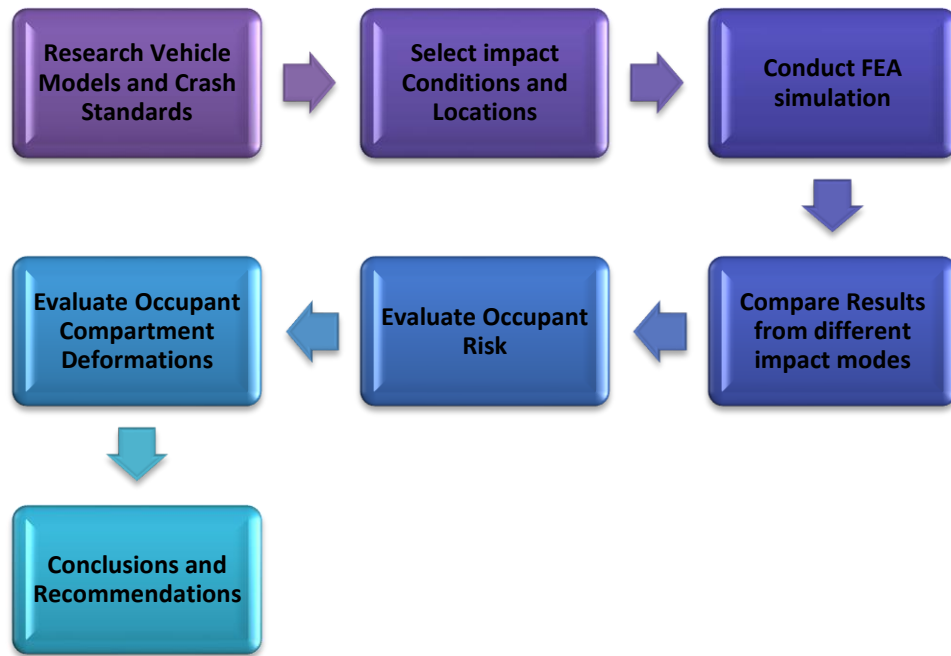


Figure 9. Overall Research Methodology

Identified Critical Crash Scenarios

The main objective of this study was to investigate the crashworthiness compatibility between no-occupant automated and passenger vehicles, for the selected scenario where the no-occupant automated vehicle is striking the passenger vehicle. This project investigates two impact modes, the side and frontal impacts. For the ADS small-sized vehicle (representation of Nuro R2) the testing nominal impact speed was limited to 40 km/hr. (25 mph) because it represented the maximum allowable operating speed for such vehicle. For other ADS vehicles which are designed to operate at higher speeds, a

testing nominal speed of 50 km/hr. (30 mph) was chosen. Specifically, two side impact test types were investigated: one aiming at the B-pillar and one at the mid-distance between A and B (mid AB pillar) (Figure 10). While the current IIHS side impact test location is the region of the B-pillar, this study concentrates on investigating other potential critical impact locations. Specifically for the side impact the Mid AB pillar location represents a less stiff geometrical characteristic and therefore potentially allows for the more occupant deformation or intrusion by the impacting vehicle.

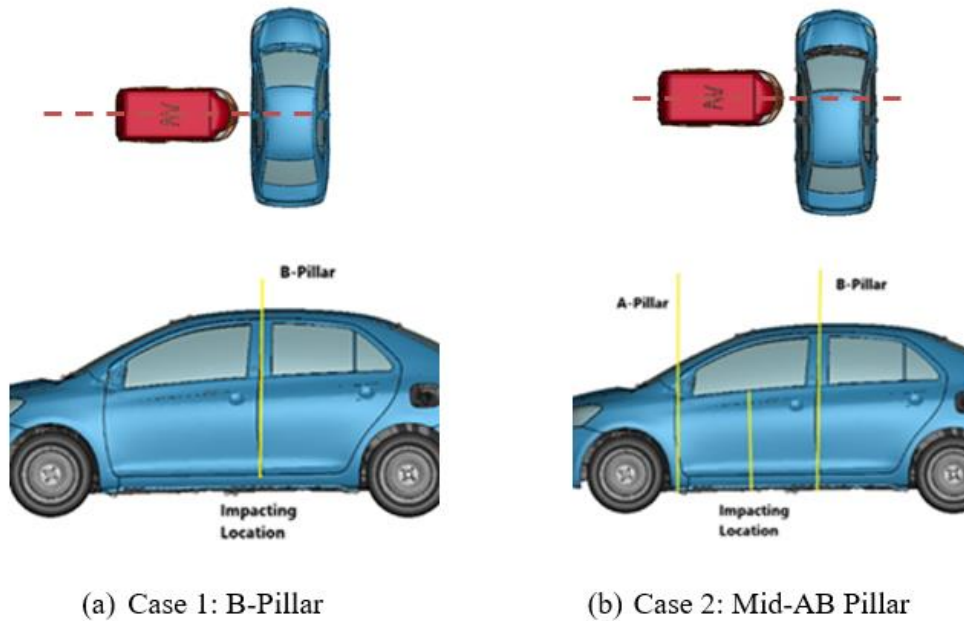


Figure 10. Impacting Locations

Two impacting scenarios were considered for the frontal impact. The equivalent of “small overlap” and “moderate overlap” IIHS impacting locations were adopted. As per IIHS testing criteria, the vehicles are impacted with a stationary barrier, which represent two similar-sized vehicles impacting each other at just under 65 km/hr. (40 mph). However, for this analysis, the passenger vehicle was considered operating at 65 km/hr.

(40 mph), while the small size ADS vehicle was considered traveling at 40 km/hr. (25 mph), its maximum operating speed. In both cases the ADS vehicle is striking the driver side of the passenger vehicle from a frontal direction. Similar case studies were conducted for Yaris vs Yaris and Yaris vs Mid-Sized ADS vehicle.

Case 1: The following case represents moderate overlap arrangement. Passenger vehicle Yaris is travelling at 65 km/hr. (40 mph) and the automated vehicle has a velocity of 40 km/hr. (25 mph) towards each other. The following images represent the arrangement in different views. The automated vehicle is moved by a magnitude of 10% (165mm) Yaris width from one of the sides as shown in the top view below.



Figure 11. Case 1. Moderate Overlap Arrangement

Case 2: This case represents small overlap configuration of the vehicle arrangement. Here the passenger vehicle Yaris is travelling at 65 km/hr. (40 mph) and the automated vehicle at 40 km/hr (25 mph). The automated vehicle is offset at 25% (412 mm) width of the Yaris from driver side.



Figure 12. Case 2. Small Overlap Arrangement

Finite Element Vehicle Models

Currently no FEA models replicating the actual geometry of NURO R2 or of any other no-occupant automated vehicle is publicly available therefore this project had to utilize existing FEA models replicating the general geometrical characteristics of such vehicles. Table 2 lists the models that were used from the George Mason University's Center for Collision Safety and Analysis (CCSA). The list is comprised of a 2010 Toyota Yaris passenger vehicle and a Silverado pick-up truck as the passenger vehicles. Coarse mesh models for both the vehicles were used for this study.

The passenger vehicle models were made by a reverse engineering process and validated against full scale crash data which conforms to MASH requirements. The Toyota Yaris has a mesh size of 12 mm for both shell and solid elements while the Silverado has 7 mm. Both quadrilateral and triangular elements were used for shell elements and for hexagonal for solid. Various materials such as rigid, piecewise linear plasticity, rubber and foam elements were used for parts such as outer geometry, engine, seats and other components. These material properties were verified using coupon testing These vehicle models were created for and used with the non-linear explicit finite element LS-Dyna

code. For this project the pre and post processing was done using LSTC Ls-Prepost modelling software.

For the no-occupant ADS vehicles, a validated FE model of traditional vehicles was selected. A skateboard type of chassis was made by excluding the seats, interior, trunk and occupant compartment which was replaced by vehicle go space [1]. The AV being electric in nature the engine and similar components were replaced by a motor and battery pack. An existing small-sized ADS vehicle already exists and is represented by Nuro R2 which is known to have a potential payload of 190 kg (420 lb.). Therefore, for the purpose of this research the equivalent of the 190 kg (420 lb.). payload was added to the FEA model of the small-sized no occupant ADS vehicle. With this decision the total mass of the FEA model of small sized ADS vehicle used in these simulations was 1340 kg (2900 lb.).

Figure 13 [Reprinted from [18]] gives a general description of small-sized ADS vehicle. The mid-sized and large-sized ADS have the same methodology involved. The no-occupant ADS vehicles are not validated against full scale crash test.

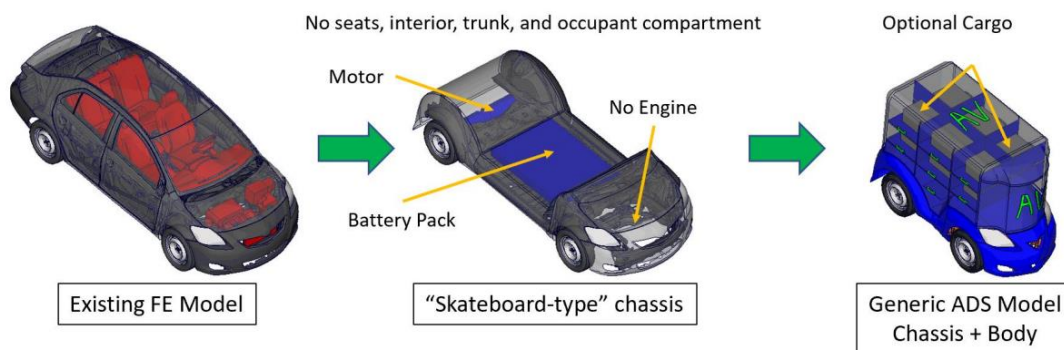


Figure 13. General development of no-occupant ADS vehicle [Reprinted from [18]]

Figure 14 shows the energy curves that were obtained during the computer simulations. The total energy during the analysis is conserved. The kinetic energy is the energy possessed by the moving vehicle and starts to decrease once the impact is made with the impacting vehicle. This energy is converted to internal, hourglass, and damping energy.

Internal energy is the energy that causes the parts in the vehicle to deform and is absorbed by the materials of the vehicle. Hourglass energy which is the energy that results from resisting the hour glassing is below the 5% recommended limit.

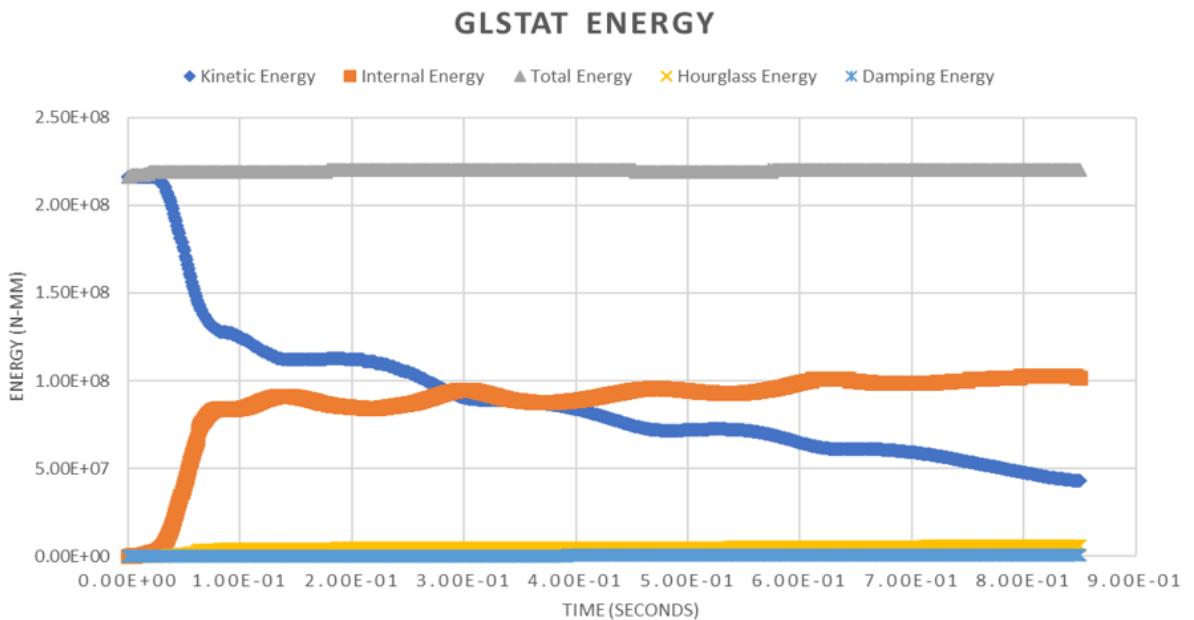


Figure 14. Energy Curve

At the time of development, the payload for both mid and large sized ADS model was not incorporated in the weight of the FEA models because no such no occupant ADS vehicles have yet been built and implemented on the roadways. Within this project

simulations involving both mid and large size no occupant ADS vehicles only considered the known gross vehicle weight.

Table 2. Finite Element Vehicle Models

| Finite Element Model | Description |
|---|---|
|  | 2010 Toyota Yaris (Coarse Mesh) <ul style="list-style-type: none"> • Gross Vehicle Weight - 1,078 kg (2,377 lb.) • Elements/Nodes/Parts – 378,376/393,165/919 • Tire Size – P185/60R15 • Body Type – Sedan 4 -Door • Engine Type – 1.5 Liter L4 DOHC 16V • Transmission – Manual |
|  | 2007 Chevrolet Silverado (Coarse Mesh) <ul style="list-style-type: none"> • Gross Vehicle Weight-2,337 kg (5,152 lb.) • Elements/Nodes/Parts – 251,400/262,061/603 • Tire Size – P245/70R17 • Body Type – 4-Door pick-up truck • Engine Type – 4.8L V8 • Transmission – M30 4 speed Automatic |
|  | Small-Sized – ADS Model <ul style="list-style-type: none"> • Gross Vehicle Weight – 900kg (2,000 lb.) • Elements/Nodes/Parts – 212,487/220,478/319 • Dimension (L*B*H) – 2.6m*1.1m*1.8m • Skateboard Type Chassis |
|  | Mid-Sized – ADS Model <ul style="list-style-type: none"> • Gross Vehicle Weight – 1,200 kg (2,645 lb.) • Elements/Nodes/Parts – 439,303/456,453/371 • Dimension (L*B*H) – 4.0m*1.7m*1.8m |
|  | Large Sized – ADS Model <ul style="list-style-type: none"> • Gross Vehicle Weight – 4,000 kg (8,000 lb.) • Elements/Nodes/Parts – 308,166/311,987/414 • Dimension (L*B*H) – 5.7m*2.0m*3.5m |

CHAPTER IV

RESULTS

Side Impact Simulation

Deformations of B-Pillar and Mid-AB Pillar

This section deals with the maximum deformations that occur between the impacting location (B-Pillar and Mid AB pillar) and the center line of the seat pan. The values measured were based on the x- axis deformation of the nodal displacement. The node selected was based on the maximum intrusion point along the x-direction.

For the mid AB- pillar the distance between the nodes at center line of the seat pan and inside of the door was used to measure the deformation.

The following figures represent the B-pillar and the part of the seat pan from where the nodes were selected for calculating the distance between them.

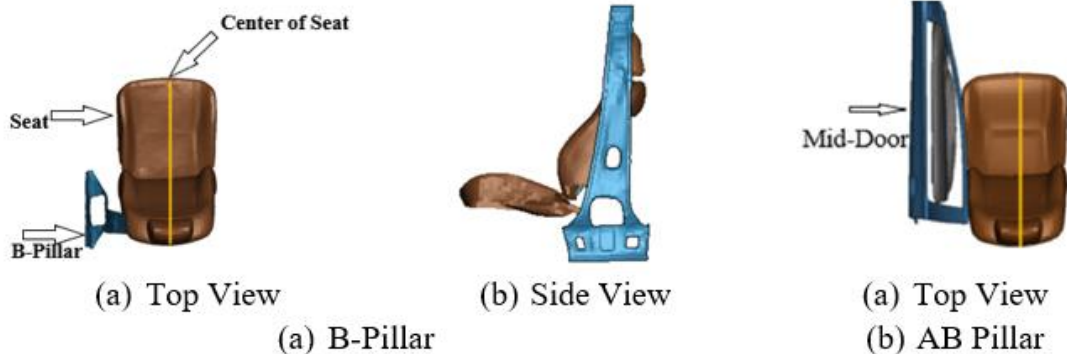


Figure 15. Measurement Locations For B-Pillar and AB Pillar



(a) Top View



(b) Back View

Figure 16. Pre-Impact Vehicle Image

Table 3 summarizes impact conditions and results of the conducted predictive impact simulations. The first column in the table summarizes the impact conditions utilized for the specific simulation, while the second column illustrates the impact configurations and the vehicles roles for each case. Screenshots of post-impact occupant compartment deformations for each simulated case are included in the third (top view) and fourth (section view) columns. These figures highlight the impacted vehicle's door deformation and the subsequent potential intrusion to the driver's seat.

Table 3. Post Impact Images of B- Pillar and AB pillar

| Impact Conditions | Impact Configurations (Top View) | Impacted Vehicle Deformation (Top View) | Impacted Vehicle Deformation (Section View) |
|---|---|--|---|
|  |  <p data-bbox="623 1663 711 1692">B-pillar</p> |  |  |

| Impact Conditions | Impact Configurations (Top View) | Impacted Vehicle Deformation (Top View) | Impacted Vehicle Deformation (Section View) |
|--|---|--|---|
| Impacting Vehicle:50 km/hr (30 mph) Impacted Vehicle: 0 km/hr |  AB-Pillar |  |  |
|  Impacting Vehicle:50 km/hr (30 mph) Impacted Vehicle: 0 km/hr |  B-pillar |  |  |
|  Impacting Vehicle:50 km/hr (30 mph) Impacted Vehicle: 0 km/hr |  B-pillar |  |  |

| Impact Conditions | Impact Configurations (Top View) | Impacted Vehicle Deformation (Top View) | Impacted Vehicle Deformation (Section View) |
|---|---|--|---|
| Impacting Vehicle: 40 km/hr (25 mph) Impacted Vehicle: 0 km/hr |  <p>AB-Pillar</p> |  |  |
|  Impacting Vehicle: 50 km/hr (30 mph) Impacted Vehicle: 0 km/hr |  <p>B-pillar</p> |  |  |
|  |  <p>B-pillar</p> |  |  |

| Impact Conditions | Impact Configurations (Top View) | Impacted Vehicle Deformation (Top View) | Impacted Vehicle Deformation (Section View) |
|--|--|--|---|
| Impacting Vehicle: 50 km/hr (30 mph) Impacted Vehicle: 0 km/hr |  AB-Pillar |  |  |

Table 4 summarizes the lateral deformations between the seat centerline and the B- or mid AB- pillar for the simulated cases. It also includes recorded results based on the IIHS deformation criteria zone for each simulated case, based on the un-deformed lateral distance (for the utilized Yaris vehicle, such undeformed distance is 35.8 cm from the B-pillar and 29.7 cm from the mid AB-pillar). Conclusions regarding the IIHS deformation criteria zone were derived based on these undeformed values.

The Toyota Yaris and Mid-Size ADS vehicles have comparable sizes, and the post deformation values fall within the “Green” zone of the IIHS deformation criteria for both the impacting locations. In comparison, for both cases of the small size ADS impacting the Yaris vehicle (against B- or mid AB-pillar), the door deformation is higher. This increase of compartment deformation is believed to be associated to the narrower shape of the small size ADS vehicle, which can penetrate more in the impacted vehicle because of a smaller engagement with both pillars, which represent more rigid structures. For the

mid AB pillar case impact configuration, the recorded post-impact distance is 8.0 cm, which represents a yellow zone when using the IIHS criteria.

Similarly, when a large size ADS (comparable to Silverado size) is considered, a higher occupant compartment deformation is recorded, because of the higher intrusion, for both B- and mid AB-pillar impacting locations. From the predictive FE simulations, it was also observed that, when a small size ADS vehicle struck the Yaris at the mid AB pillar location, the post-impact movement of the entire Yaris vehicle was lower than the one recorded when the same Yaris vehicle was impacted by another Yaris or even a larger pick-up truck. The smaller Yaris movement indicates that the kinetic energy from the impact is mostly dissipated by deforming the Yaris occupant compartment. This, in turn, is an indication that the impacting ADS vehicle does not have much crumple zone to help with the dissipation of impacting energy, which, instead, is transmitted mostly to the impacted vehicle.

The resultant B pillar and MID-AB Pillar values for the small sized ADS vehicle appears to be considerably different, potentially due to the very narrow, bullet-like, shape of the small sized ADS vehicle. Based on the proposed methodology and on the accessible information and FEA models, it appears that there is a potential for automated vehicles to be designed to account for the need of crashworthiness compatibility with existing passenger vehicles.

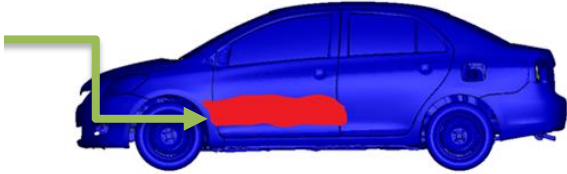
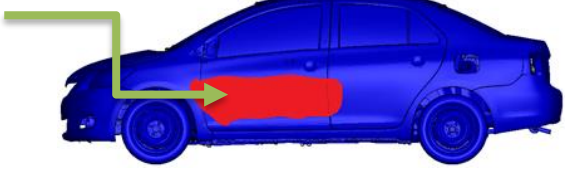
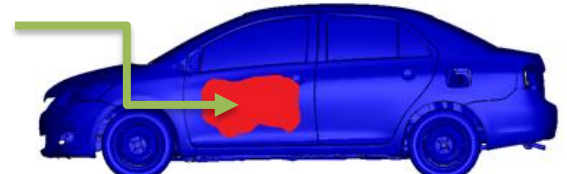
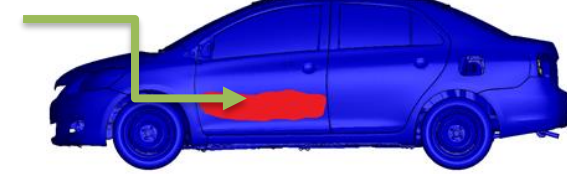
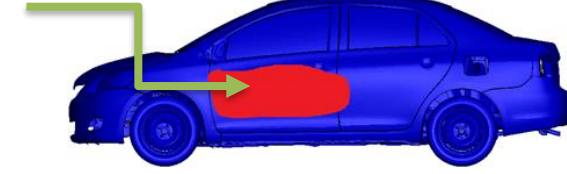
Table 4. B- and Mid AB-Pillar deformation values

| Impacted Vehicle | Impacting Vehicle | Lateral post-impact distance between seat centerline and B-pillar (cm) | Lateral post-impact distance between seat centerline and AB-pillar (cm) |
|------------------|-------------------|--|---|
| Yaris | Small-Sized ADS | 22.4 | 8.0 |
| Yaris | Mid-Sized ADS* | 27.3 | 20.3 |
| Yaris | Large-Sized ADS* | 18.7 | 10.4 |
| Yaris | Yaris | 26.9 | 20.9 |
| Yaris | Silverado | 21.5 | 12.3 |

* Weight does not include the payload

The following figures in Table 5 represent the post impact deformation of the impacted vehicle for the Mid AB pillar location. The highlighted red area indicates the region on the door where the impact energy is concentrated. Although the impacting location was at the center but owing to the difference in the sizes of the vehicle's deformation zone is different. One key observation is that the impact location of the small size and mid-size ads vehicle is more concentrated compared to other vehicles based on the width of the vehicles. This means there will be more deformation on the door and subsequently more chances of injury to the occupant. However, for the two passenger vehicles the region is wide and covers some part of A and B pillar which might reduce the overall deformation and thus less effect on the occupant.

Table 5. AB Pillar door intrusion area

| Impacting Vehicle | Impacted Vehicle | Image |
|-------------------|------------------|---|
| Yaris | Yaris | <p data-bbox="646 491 776 596">Impacting vehicle</p>  |
| Silverado | Yaris | <p data-bbox="646 745 776 850">Impacting vehicle</p>  |
| Small-Size ADS | Yaris | <p data-bbox="646 976 776 1081">Impacting vehicle</p>  |
| Mid-Size ADS | Yaris | <p data-bbox="646 1230 776 1335">Impacting vehicle</p>  |
| Large-Size ADS | Yaris | <p data-bbox="646 1482 776 1587">Impacting vehicle</p>  |

Frontal Impact Simulations

Moderate and Small Overlap Impact Simulations

One key observation from Table 6 is that although Yaris and Mid-Sized ADS have similar dimensions the damage (intrusion) is more for the latter case for both small and moderate overlap impacting configurations.

Table 6 summarizes impact conditions and results of the front small and moderate overlap impact simulations. The first column in the table summarizes the impact conditions utilized for the specific simulation, while the second column illustrates the impact configurations and the vehicles roles for each case. Screenshots of post-impact occupant compartment deformations for each simulated case are included in the third (top view) column. These figures highlight the impacted vehicle's interior parts as evaluated by the IIHS criteria mentioned in Figure 8.

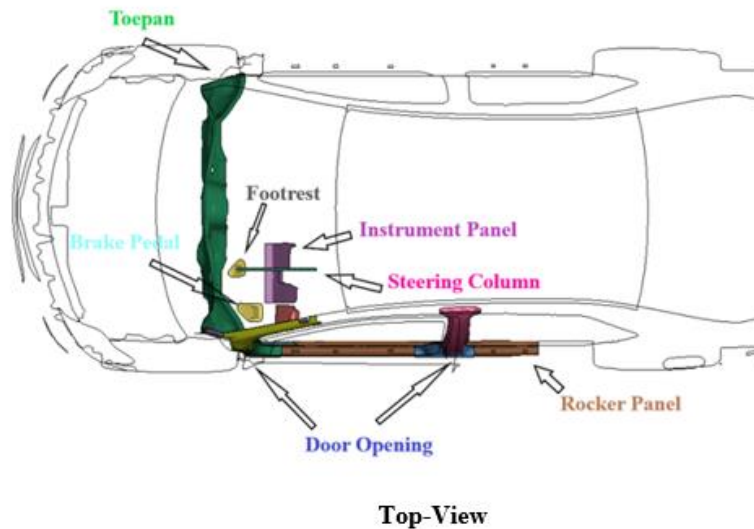


Figure 17. Pre-Impact Image

One key observation from Table 6 is that although Yaris and Mid-Sized ADS have similar dimensions the damage (intrusion) is more for the latter case for both small and moderate overlap case.

Table 6. Post Impact Images of Small and Moderate Overlap

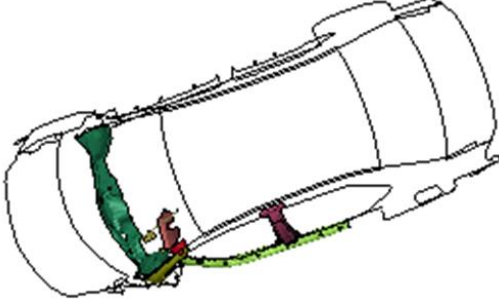
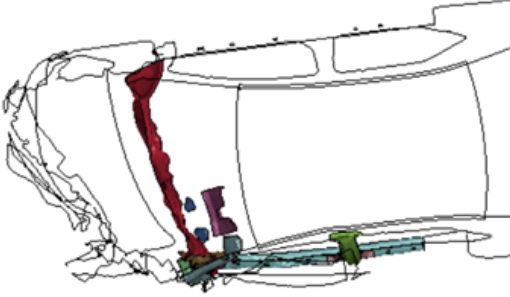
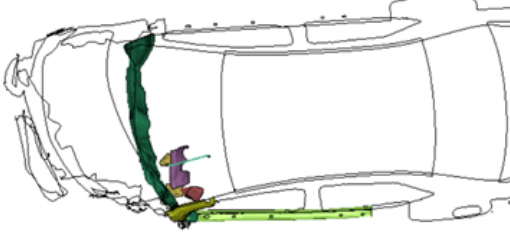
| Impact Conditions | Impact Configurations (Top View) | Impacted Vehicle Deformation (Top View) |
|--|---|--|
| Yaris:40 mph Yaris:40 mph |  <p data-bbox="654 1016 808 1047">Small Overlap</p> |  |
| |  <p data-bbox="634 1388 829 1419">Moderate Overlap</p> |  |
| Small-Sized ADS: 25 mph Yaris: 40 mph |  <p data-bbox="654 1745 808 1776">Small Overlap</p> |  |

Table 6 (continued)

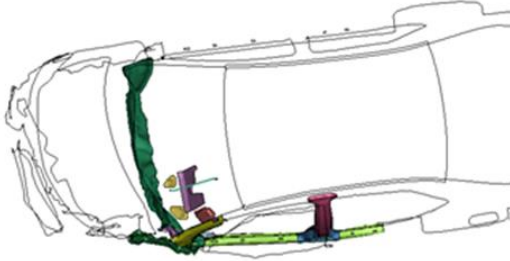
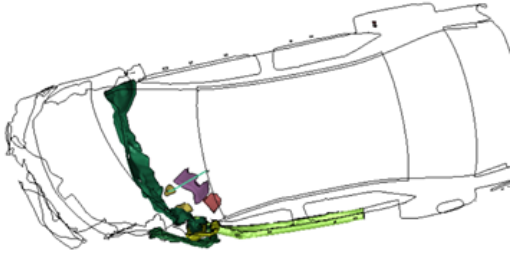
| Impact Conditions | Impact Configurations (Top View) | Impacted Vehicle Deformation (Top View) |
|-----------------------|---|--|
| |  <p>Moderate Overlap</p> |  |
| Mid-Sized ADS: 40 mph |  <p>Small Overlap</p> |  |
| Yaris: 40 mph |  <p>Moderate Overlap</p> |  |

Table 7 and Table 8 include Occupant Impact Velocities (OIV's) and Ride Down Acceleration (RDA) for the accelerometer at the Center of gravity of Yaris. The values were calculated using the Test Risk Assessment Program (TRAP) and Figure 18 shows the coordinate system used. The negative value in the tables indicate the direction of the occupant inside the Yaris. These results indicate that the occupant will experience more

impact velocity for the Mid-Sized ADS vehicle compared with other two vehicles. However, the difference is very little.

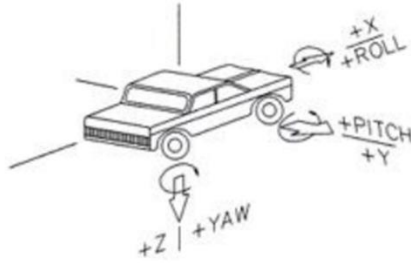


Figure 18. TRAP Coordinate System

Table 7. Small Overlap OIV and Ride Down Acceleration values

| Impacted Vehicle | Impacting Vehicle | Occupant Impact Velocity (OIV) (m/s) | | Ride-Down Acceleration (g) | |
|------------------|-------------------|--------------------------------------|------|----------------------------|------|
| | | X | Y | X | Y |
| Yaris | Yaris | 13.6 | -3.0 | -2.3 | -4.6 |
| Yaris | Small size ADS | 14.4 | -2.9 | 4.2 | -6.0 |
| Yaris | Mid-Size ADS | 16.2 | -3.5 | -5.4 | 6.0 |

Table 8. Moderate Overlap OIV and Ride Down Acceleration values

| Impacted Vehicle | Impacting Vehicle | Occupant Impact Velocity (OIV) (m/s) | | Ride-Down Acceleration (g) | |
|------------------|-------------------|--------------------------------------|------|----------------------------|------|
| | | X | Y | X | Y |
| Yaris | Yaris | 16.7 | -2.8 | -7.1 | 4.6 |
| Yaris | Small size ADS | 15.3 | -2.4 | -2.8 | -7.5 |
| Yaris | Mid-Size ADS | 17.5 | -3.2 | -7.0 | -4.9 |

Table 9 and Table 10 include the intrusion of the locations for both small and moderate overlap respectively. These locations are measured from the vehicle door striker.

The colors represent the different zones as mentioned in Figure 8 [adapted from [iihs.org]

[9][10]. For both the impact locations passenger vehicle and small sized ADS vehicle give good ratings with couple of them under the Yellow i.e., acceptable range. However, the mid-sized vehicle gives results in all the different zones with around 50% of them in red and marginal zone indicating that the damage done is quite significant.

Table 9. Small Overlap Intrusion Measurements

| Impacted vehicle | Impacting Vehicle | Measuring Locations (cm) | | | | | | | |
|------------------|-------------------|--------------------------|--------------|-------------|--------------|-----------------|--------------------|------------|-----------------------|
| | | Lower Hinge Pillar | Left Toeapan | Brake Pedal | Rocker Panel | Steering Column | Upper Hinge Pillar | Upper Dash | Left Instrument Panel |
| Yaris | Yaris | 6 | 21 | 4 | 4 | 0 | 4 | 1 | 10 |
| Yaris | Small-Sized ADS | 5 | 21 | 2 | 1 | 0 | 5 | 1 | 6 |
| Yaris | Mid-Sized ADS | 22 | 34 | 10 | 12 | 2 | 22 | 13 | 22 |

Table 10. Moderate Overlap Intrusion Measurements

| Impacted Vehicle | Impacting Vehicle | Measuring Locations Intrusion (cm) | | | | | |
|------------------|-------------------|------------------------------------|----------------|---------------|-------------|-----------------------|--------------|
| | | Left Toeapan | Center Toeapan | Right Toeapan | Brake Pedal | Left Instrument Panel | Door Opening |
| Yaris | Yaris | 16 | 4 | 2 | 6 | 0 | 10 |
| Yaris | Small-Sized ADS | 17 | 1 | 0 | 2 | 0 | 11 |
| Yaris | Mid-Sized ADS | 39 | 25 | 5 | 16 | 15 | 16 |

CHAPTER V

CONCLUSIONS

Discussion

Detailed FEA models of passenger vehicles and of no-occupant automated delivery vehicles were utilized to conduct impact computer simulations. Such computer simulations represented the condition of a passenger vehicle being impacted by other vehicle types at different impacting conditions, with the objective to understand whether vehicle crashworthiness compatibility needs to yet be considered for cases where impacting no-occupant automated vehicles are considered. The simulations were performed to assess the difference in the geometry and shape of the novel no-occupant automated vehicles equipped with ADS compared with the traditional passenger vehicles. The results suggest that, for side impact cases, the deformation of the occupant compartment of the passenger vehicle was different when an ADS vehicle was the impacting vehicle, for both mid-AB pillar and B-pillar impact configurations. One key observation is the upcoming ADS vehicles could have higher mass and speed than used in this study and that means the intrusion will be more which ultimately can increase the risk of occupant injury especially in the Mid AB pillar case. Increased mass and higher speeds will increase the kinetic energy of the vehicle which ultimately will increase the amount of force transmitted to the occupant compartment of the traditional passenger vehicles. Moreover, since these no-occupant automated vehicles have more bullet shape structure the intrusion in the impacted area will be more localized increasing the chances of penetration into the impacted vehicle. When compared with the passenger vehicle the no-occupant vehicles do not have a crumple zone which can significantly lead to increased amount of force transmitted specially in

the side impact scenarios as there is no protection in the side of passenger vehicle. This force exemplifies even more in case of the Mid AB pillar impact as the section is much weaker structurally. In the conventional IIHS criteria there is B-pillar which does offer a little bit more protection but nothing such exists in the middle of the door. Another point to notice is that when the impact is at Mid AB pillar the impact region is below the chest of the occupant and more near the legs. Although the vehicles are equipped with side airbags, but they protect only the head and do not go below the side window providing no support to the legs of the occupant.

For the frontal impact cases, both small and moderate overlap tests showed deformations within the acceptable values, due to the limitation in speed for the small -sized ADS. However, for the Mid-Sized ADS which has a geometry comparable to Yaris passenger vehicle the deformations were quite significant and overall, there were more “Poor” and “Marginal” regions rather than “Good” or “Acceptable” for both moderate and small overlap configurations. The intrusion in the toepan for both the configurations was quite significant. This toepan is the region which is directly in front of the legs of the driver in the vehicle and the high value of intrusion can cause severe injuries. Moreover, the airbags are near the steering wheel and only cover the head during the impact. Seat belt helps to increase the distance after impact of the occupant and thus reduce the impacting force and decelerating effect of the chest. However, there is no such mechanism for the legs. These results were done at no payload and 40 mph velocity however in real life the MID-sized ADS is expected to have higher mass and higher velocity which will enhance the intrusion and can cause more injuries to the occupant. These values contrast with the case between two regular passenger vehicles where the regions were in the “Good” zone.

As per the conservation of energy principle during the impact kinetic energy of the moving vehicle is converted to the work done by the impact force.

Mathematically,

$$\text{Kinetic Energy} = (m * v^2)/2$$

$$\text{Work Done} = F * d$$

Kinetic Energy = Work Done

$$F = (m * (v^2))/2 * d$$

Where,

$$F = \text{Impact force}$$

$$m = \text{mass}$$

$$v = \text{velocity}$$

$$d = \text{distance moved after impact}$$

Based on this analogy the impact force is proportional to the mass and square of the velocity. In general, the no-occupant automated vehicles are expected to have more mass and higher velocities. Moreover, the absence of crumple zone will add to the amount of force going towards the impacted vehicle making the situation more critical.

Recommendations

The analysis results suggest that the no-occupant automated vehicles cause more penetration due compact geometry and absence of crumple zone, and the energy of impact ultimately is taken by the other vehicle for the side impact testing compared with a passenger vehicle. The occupant risks calculated were higher for the mid AB pillar compared with B-pillar. However more study needs to be conducted for the no-occupant automated vehicle fleet.

Moreover, such vehicles are expected to have higher mass and velocity that can greatly influence the deformation and occupant injuries.

Full scale crash tests need to be conducted at the proposed impacting conditions to verify the results that were predicted through simulations. The no-occupant automated finite element vehicle models used in the analysis need to be calibrated and modified if needed. If these calibrated simulated results still indicate a non-crashworthiness compatibility penetration, then a proper design modification are needed for these vehicles to verify and quantify how these modifications are development of impact testing criteria and evaluation criteria to evaluate crashworthiness compatibility of existing non ads vehicle. Some of the possible modifications include including crumple zones, modifying material properties that can absorb impact force within the automated vehicle and reconsider the geometry to redistribute the load evenly.

REFERENCES

1. Reichert, R., Marzougui, D., & Kan, C.-D. (2020, June). Crash simulations between non-occupied automated driving systems and roadside hardware (Report No. DOT HS 812 871). National Highway Traffic Safety Administration.
2. *How crumple zones work.* <https://auto.howstuffworks.com/car-driving-safety/safety-regulatory-devices/crumple-zone.htm>.
3. *Automated Driving Systems: A Vision for safety* DOT HS 812 442; September 2017. https://www.nhtsa.gov/sites/nhtsa.gov/files/documents/13069a-ads2.0_090617_v9a_tag.pdf.
4. *Self-driving vehicles could struggle to eliminate most crashes.* <https://www.iihs.org/news/detail/self-driving-vehicles-could-struggle-to-eliminate-most-crashes>. June 4, 2020.
5. *About Our Tests.* <https://www.iihs.org/ratings/about-our-tests>.
6. Raul A. Arbelaez, Becky C. Mueller, Matthew L. Brumbelow, Eric R. Teoh. Next Steps for the IIHS Side Crashworthiness Evaluation Program. Insurance Institute for Highway Safety (IIHS).
7. Brumbelow, Matthew & Mueller, Becky & Arbelaez, Raul & Kuehn, Matthias. (2017). Investigating potential changes to the IIHS side impact crashworthiness evaluation program.
8. *Side Impact Crashworthiness Evaluation Crash Test Protocol (Version X).* https://www.iihs.org/media/ebc9bd1f-2ca4-4fb9-b96e-f4165f331943/Jil-Xg/Ratings/Protocols/current/test_protocol_side.pdf.
9. *Moderate Overlap Frontal Crashworthiness Evaluation Crash Test Protocol (Version XIX).* https://www.iihs.org/media/f70ff6eb-d7a1-4b60-a82f-e4e8e0be7323/XPsNNA/Ratings/Protocols/current/test_protocol_moderate.pdf

10. *Small Overlap Frontal Crashworthiness Evaluation Crash Test Protocol (Version VII)*
https://www.iihs.org/media/ec54a7ea-1a1d-4fb2-8fc3-b2e018db2082/1A5oYw/Ratings/Protocols/current/small_overlap_test_protocol.pdf
11. Michie, D. J., 1981, "Collision Risk Assessment Based on Occupant Flail-Space Model," *Transportation Research Record*, pp. 1–9.
12. Ross, H.E., Sicking, D.L., Zimmer, R.A., and Michie, J.D., Recommended Procedures for the Safety Performance Evaluation of Highway Features, National Cooperative Research Program (NCHRP) Report 350, Transportation Research Board, Washington, D.C., 1993.
13. *Manual for Assessing Safety Hardware (MASH)*, American Association of State Highway and Transportation Officials (AASHTO), Washington, D.C., 2016.
14. *Issues in Autonomous Vehicle Testing and Deployment*.
<https://fas.org/sgp/crs/misc/R45985.pdf>
15. www.nuro.ai
16. <https://en.wikipedia.org/wiki/Einride>
17. <https://www.zoox.com/>.
18. <https://www.ccsa.gmu.edu/wp-content/uploads/2019/11/2019-generic-small-ads-vehicle-v1.pdf>